Bulgarian Chemical Communications, Volume 50, Special issue H (pp. 109–115) 2018

Properties of mechanochemically synthesised N-doped Fe_2O_3-ZnO mixed oxide

N. G. Kostova*[1], M. Fabian[2], E. Dutkova[2], N. Velinov[1], Y. Karakirova[1], M. Balaz[2]

[1] *Institute of Catalysis, Bulgarian Academy of Sciences, 1113 Sofia, Bulgaria*
[2] *Institute of Geotechnics, Slovak Academy of Sciences, 04001 Kosice, Slovakia*

Received: February 02, 2018; Revised: April 13, 2018

This work reports synthesis and characterisation of N-doped Fe_2O_3-ZnO mixed oxide and the ability of this material to decolourise Methyl Orange organic dye in aqueous solution under visible light irradiation. The photocatalytic material was prepared using eco-friendly simple mechanochemical synthesis. The photocatalysts were characterised by X-ray diffraction (XRD), UV-vis diffuse reflectance spectroscopy (DRS), photoluminescence spectroscopy (PL), and electron paramagnetic resonance (EPR) methods as well as Mössbauer spectroscopy. XRD analysis showed that employed mechanochemical synthesis promoted changes in crystallite size. A lower band gap was observed. The lower band gap and an improved photocatalytic activity under visible light irradiation of the mechanochemically synthesised nitrogen-doped Fe_2O_3-ZnO mixed oxide were registered in comparison with ZnO. A lower intensity in the PL spectra of N-Fe_2O_3-ZnO confirmed better separation and lower electron-hole recombination rate and accordingly higher photodecolourisation performance than initial ZnO.

Key words: mechanochemistry, photocatalysis, dye discolouration, Methyl Orange.

INTRODUCTION

Heterogeneous photocatalysis has been widely investigated as a technique for environmental detoxification in both water and air [1]. Semiconductors are widely studied as photocatalysts for degradation of organic contaminants in wastewaters [2]. Many semiconductors such as metal oxides and metal sulphides have been employed to study photocatalytic reduction of pollutants in water [3]. ZnO is often used as a solid photocatalyst [4]. The zinc oxide has higher efficiency in photocatalytic performance than TiO_2 due to its high quantum efficiency [5]. Zinc oxide in the wurtzite phase is the most used metal oxide as photocatalyst due to its electronic band structure. ZnO is a wide band gap semiconductor (E_g = 3.37 eV) that utilises only the UV portion (about 5%) of solar energy. Therefore, considerable effort has been applied to extend the response of ZnO to photodegradation of pollutants by visible-light irradiation [6]. This disadvantage is overcome in two ways, namely: by coupling with another metal oxide [7] or by doping with non-metal [8].

Hematite (α-Fe_2O_3) is a promising candidate for photocatalytic applications due to its narrow band gap of 2.2 eV [9]. Furthermore, hematite absorbs light up to 600 nm, collects up to 40% of the solar spectrum energy. Being stable in most aqueous solutions, it is one of the cheapest available semiconductor materials [10]. Development of coupled semiconductor photocatalysts is a significant advancement in catalytic functional materials [11]. Mixed oxides show a considerably higher photocatalytic activity for dye removal from wastewater under visible light irradiation than that of a single semiconductor [12]. The mixed oxides have been fabricated by different techniques such as hydrothermal-thermal decomposition [11], sol-gel [12], reflux condensation [13], homogeneous precipitation [14], and mechanochemical methods [15]. High-energy milling is one of the most powerful techniques for synthesis of photocatalysts [16].

Nitrogen doping represents an important strategy to modulate the optical and photocatalytic properties of metal oxides [17]. Nitrogen doping is more effective than carbon/sulphur doping to achieve a high visible-light response [18]. Highly intensive homogenisation by milling of the mixture of interacting components makes mechanochemical synthesis easier [19].

In this work N-doped Fe_2O_3-ZnO mixed oxide prepared by mechanochemical synthesis was investigated to evaluate photodecolourisation of Methyl Orange (MO) as a dye model system. Here, N-doping of mixed Fe_2O_3-ZnO oxide was studied as a low cost alternative to enhance ZnO photoactivity in visible light irradiation by slowing down photogenerated charge recombination.

* To whom all correspondence should be sent
E-mail: nkostova@ic.bas.bg

EXPERIMENTAL

Materials

Commercial ZnO was purchased from Himsnab Company (Bulgaria). Hematite (Aldrich) and ammonia reagents of analytical grade were used without further purification. Samples of N-doped Fe_2O_3-ZnO mixed oxide were prepared by mechanochemical synthesis using a high-energy planetary ball mill Pulverisette 6 (Fritsch, Germany). The precursors were milled for 0.5 h at 550 rpm in ambient atmosphere using a chamber (250 cm^3) with 21 balls (10 mm in diameter) both made of zirconia. The ball-to-powder mass ratio was 40:1. After milling, the powdered mixture was calcined at 673 K in air for 2 h.

Methods of investigation

X-ray diffraction (XRD) patterns were recorded on a D8 Advance diffractometer (Brucker, Germany) using CuKα radiation. Diffraction data were collected over angular range of $20° < 2\Theta < 65°$ with steps of 0.02° and a counting time of 9 s/step. Commercial Diffrac^{plus} Topas was utilised for Rietveld analysis.

Diffuse reflectance UV-vis spectra for evaluation of photophysical properties were recorded in the diffuse reflectance mode and transformed to absorption spectra through the Kubelka-Munk function [20]. A Thermo Evolution 300 UV-vis spectrophotometer, equipped with a Praying Mantis device with Spectralon as the reference was used.

Photoluminescence (PL) spectra at room temperature were acquired at right angle on a photon counting spectrofluorometer PC1 (ISS) with a photoexcitation wavelength of 325 nm. A 300-W xenon lamp was used as the excitation source. For measuring the PL intensity, the powders were suspended in absolute ethanol.

Room temperature Mössbauer spectra were registered by measurements with a Wissel (Wissenschaftliche Elektronik GMBN, Germany) electromechanical spectrometer working in a constant acceleration mode. A 57 Co/Rh (activity = 50 mCi) source and α-Fe standard were used. Parameters of hyperfine interaction, such as isomer shift (δ), quadrupole splitting (Δ), magnetic hyperfine field (*B*), line widths (FWHM), and relative weight (*G*) of partial components in the spectra were determined according to Ref. [21].

EPR spectra were recorded at room temperature on a JEOL JES-FA 100 EPR spectrometer operating in the X-band equipped with a standard TE_{011} cylindrical resonator. The samples were placed in quartz tubes and fixed in the cavity centre. The instrumental settings using the above spectrometer were modulation frequency of 100 kHz, sweep 500 mT, time constant 0.3 s, sweep time 2 min, microwave power 1 mW, and amplitude of the magnetic field modulation of 0.2 mT.

Photocatalytic test

Methyl Orange adsorption on initial ZnO and mechanochemically synthesised Fe_2O_3-ZnO and N-doped Fe_2O_3-ZnO samples was measured in the dark. In each experiment, 100 mg of sample were added to dye aqueous solution. Then the suspension was magnetically stirred for 30 min at room temperature in the dark in the absence of oxygen to attain adsorption-desorption equilibrium [22]. The photocatalytic activity of all samples was determined by photodecolourisation of Methyl Orange organic dye under visible light illumination. Moreover, 0.10 g of prepared photocatalyst was suspended in 100 ml of MO solution. The obtained mixture was subjected to stirring in the dark for 30 min to achieve adsorption-desorption equilibrium. Then, the mixed suspension was kept under visible light illumination. At a given time interval, 6 ml of mixed suspension was sampled and centrifuged to eliminate the photocatalyst. The residual concentration of MO was estimated at 463 nm using a SPEKOL 11 (Carl Zeiss Jenna) spectrophotometer.

RESULTS AND DISCUSSION

X-ray data analysis

Powder X-ray diffraction (XRD) analysis was used to identify the crystal phase of the samples. The XRD patterns of pure ZnO and mechanochemically synthesised N-doped Fe_2O_3-ZnO samples after heat treatment are shown in Fig. 1.

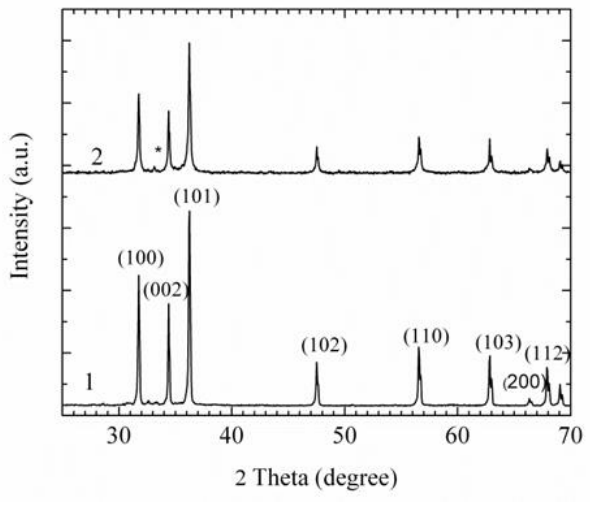

Fig. 1. XRD pattern of initial ZnO (1) and mechanochemically synthesised N-Fe_2O_3-ZnO sample (2).

Identification of the registered peaks was performed using the JCPDS card 36-1451 for ZnO. The three most intensive peaks at $2\Theta = 31.74$, 34.38, and 36.2° were assigned to (100), (002), and (101) reflections of ZnO, indicating that the samples were of hexa-gona wurtzite structure. For the mechanochemically synthesised N-Fe_2O_3-ZnO sample an additional diffraction peak of α-Fe_2O_3 appeared at $2\theta = 33.15°$ reflection (104) that is typical of hematite (JCPDS card No 33-0664). The XRD pattern confirmed the formation of nanocrystalline mixed oxide. No peaks consistent with another N-containing phase were detected in the XRD pattern of mechanochemically synthesised sample. The peak intensities of the mechanochemically synthesised sample were lower along with certain broadening (Fig. 1). Thus, mechanochemical synthesis promotes changes in crystallite size of the ZnO material. The average crystallite size of ZnO decreased from 168 nm to about 90 nm.

Diffuse reflectance spectra

UV-vis diffuse reflectance spectra are shown in Fig. 2. A pure ZnO sample could absorb only ultraviolet light. A spectrum of N-doped Fe_2O_3-ZnO sample demonstrated a reflectance, covering wavelengths from 200 to 800 nm. A decrease of the reflectance was observed for doped mixed oxide compared with pure ZnO.

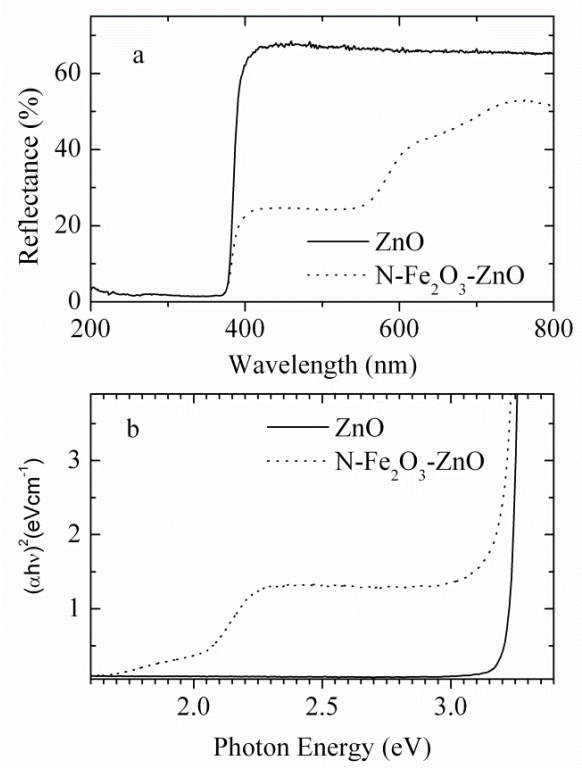

Fig. 2. Diffuse reflectance spectra (a) and plot of $(\alpha h\nu)^2$ versus energy (b) of pure ZnO and mechanochemically synthesised N-doped Fe_2O_3-ZnO sample.

The reflectance edge of mechanochemically synthesised N-doped Fe_2O_3-ZnO sample manifested a red shift. Electronic interactions between ZnO and Fe_2O_3 induced a shift of the band gap absorption to longer wavelengths [23]. This result suggested that the N-doped Fe_2O_3-ZnO sample had a potential for photocatalysis using the visible part of the spectrum.

The band gap energy of all samples was calculated from the diffuse reflectance spectra by performing a Kubelka-Munk analysis using the following equation:

$$F(R) = (1-R)^2/2R, \quad (1)$$

where R is the diffuse reflectance. According to this function the band gap energy can be obtained by plotting the $F(R)^2$ vs. the energy in electron volts. The linear part of the curve was extrapolated to $F(R)^2 = 0$ to calculate the direct band gap energy. The results are presented in Fig. 2b. The band gap of the initial ZnO was 3.38 eV, whereas that of the mechanochemically synthesised N-doped Fe_2O_3-ZnO sample was 1.98 eV. A red shift was attributed to sp-d exchange interactions between the band electrons and the localised d electrons of Fe ions.

Photoluminescence

Because of its high sensitivity and nondestructive nature, photoluminescence (PL) spectroscopy was applied to obtain significant information about the structure of active sites of metal oxides [24]. Room temperature PL spectra of samples were also recorded to study sample defects. Fig. 3 shows PL spectra of the starting ZnO and prepared N-Fe_2O_3-ZnO samples excited by UV-ray wavelength of 325 nm (photon energy of 3.81 eV) that usually leads to ZnO emission. They exhibit a strong ultraviolet emission at 391 nm and a weak green-yellow emission at 530 nm. The UV emission is attributed to a free excitonic recombination through free excitons transition process [25].

In the spectrum of mechanochemically synthesised N-Fe_2O_3-ZnO sample, the PL intensity drastically decreased while the line width increased with a shift of emission maximum towards longer wavelengths. This spectrum could be decomposed into PL bands, one in the green, and another in the yellow region. The green luminescence arises from a radiative recombination involving an intrinsic defect located at the surface [26]. The peak intensity of PL spectra correlate with the recombination rate of electron-hole pairs. As the PL emission is the result of the recombination of excited electrons and holes, a lower PL intensity indicates a decrease in recombination rate and thus higher photocatalytic activity [27]. Therefore, it is deduced that the Fe^{3+}

ions trapped the photogenerated electrons, while nitrogen trapped the photogenerated holes, leading to enhanced quantum efficiency and photocatalytic activity [28].

An increase in oxygen vacancies that acted as electron donors in the ZnO lattice promoted better charge separation. Reduction of emission intensity signified a high efficiency of charge separation and transfer between N, Fe_2O_3, and ZnO.

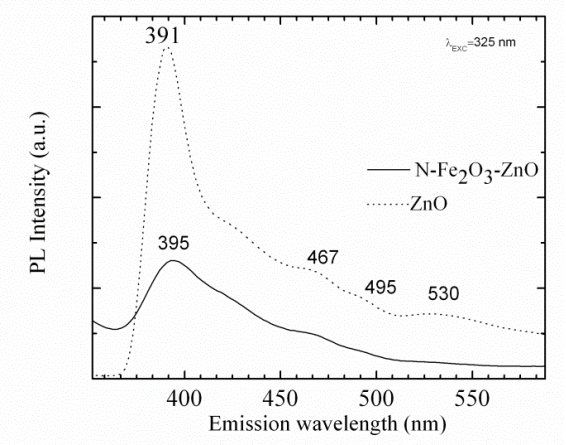

Fig. 3. Photoluminescence spectra of initial ZnO (dot line) and mechanochemically synthesised N-Fe_2O_3-ZnO sample (solid line).

Mössbauer spectroscopy

57Fe Mössbauer spectra of initial α-Fe_2O_3 and mechanochemically synthesised N-Fe_2O_3-ZnO samples are displayed in Fig. 4 and consequent parameters of the materials are listed in Table 1.

The Mössbauer spectrum of pure Fe_2O_3 was fitted with one sextet with IS of 0.37 mm/s, H_{eff} = 51.5 T, and a negative QS which could be assigned to hematite. The result agrees well with the data from XRD analysis. The Mössbauer spectrum of the N-Fe_2O_3-ZnO sample is a combination of sextet and doublet (Table 1). Sextet parameters respond to octahedrally coordinated Fe^{3+} ions in antiferromagnetic hematite, while doublet ones reconcile to Fe^{3+} ions in octahedral coordination in paramagnetic or superparamagnetic oxide phase. An approximative phase ratio in the sample can be assumed based on the ratio between calculated relative weights of the components G (Table 1). The doublet with QS = 0.75 mm/s can be ascribed to α-Fe_2O_3 particles, the sizes of which are below the critical one for the transition of ferromagnetic to superparamagnetic behaviour [29].

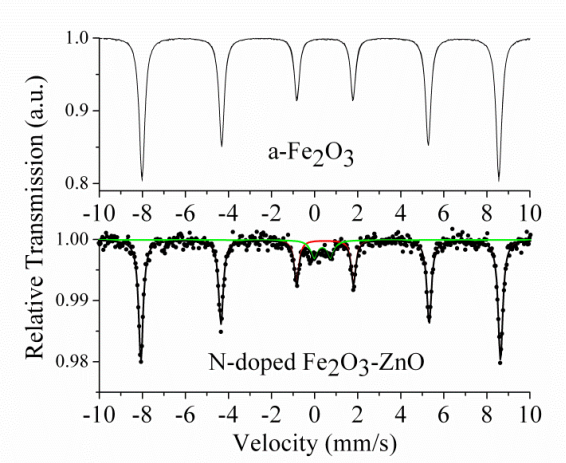

Fig. 4. Mössbauer spectra of initial α-Fe_2O_3 and N-Fe_2O_3-ZnO samples.

Electron paramagnetic resonance spectroscopy

Typical EPR spectra of initial ZnO and mechanochemically synthesised N-doped ZnO and N-Fe_2O_3-ZnO samples are given in Fig. 5. The EPR spectrum of pure Fe_2O_3 is characterised by a wide line with g value of 2.6997. This line is due to paramagnetic Fe^{3+} ions. The reason for the very wide signal and movement of the g factor to lower magnetic field in comparison with that reported in the literature is a high concentration of ferrous ions and their spin-spin interactions.

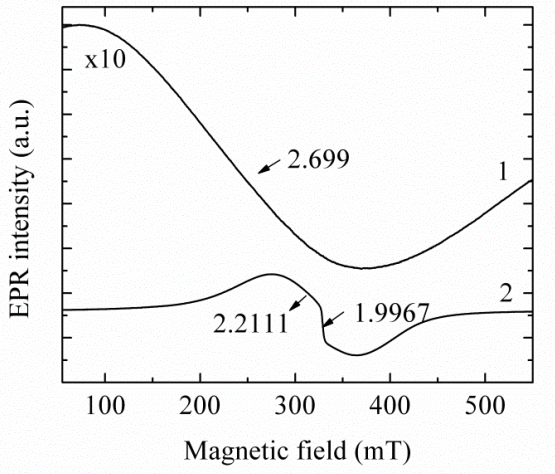

Fig. 5. EPR spectra of α-Fe_2O_3 (1) and mechanochemically synthesised N-Fe_2O_3-ZnO sample (2).

Table 1. Room temperature Mössbauer parameters

Sample	Component	IS, mm/s	QS, mm/s	H_{eff}, T	FWHM, mm/s	G, %
α-Fe_2O_3	Sx-α-Fe_2O_3-Fe^{3+}	0.37	−0.21	51.5	0.30	100
N-Fe_2O_3-ZnO	Sx-α-Fe_2O_3-Fe^{3+}	0.38	−0.20	51.9	0.26	90
	Db-Fe^{3+}	0.36	0.75	-	0.40	10

The EPR spectrum of mechanochemically prepared N-Fe_2O_3-ZnO sample can be regarded as superposition of two overlapping EPR signals. One of the signals is wide with g factor around 2.211 and ΔH = 87.74 mT due to octahedrally coordinated Fe^{3+} ions of more finely dispersed iron oxide species [30]. The other signal with ΔH = 4.48 mT and g value of 1.9967 is generally attributed to an unpaired electron trapped on an oxygen vacancy site [31].

Photocatalytic activity

The photocatalytic activities of the samples were evaluated by photodecolourisation of MO in aqueous solutions under visible light irradiation. A preliminary test showed that the direct photolysis process is very slow and can be considered negligible in the same time. Fig. 6a shows decolourisation of MO as a function of irradiation time for the pure ZnO and mechanochemically synthesised N-Fe_2O_3-ZnO samples. Compared to undoped ZnO, the N-Fe_2O_3-ZnO sample showed a considerably enhanced photoactivity. The N-Fe_2O_3-ZnO sample demonstrated discoloration efficiency of 42% in 120 min irradiation that was higher than the ZnO efficiency for the same time duration. The electronic configuration obtained after coupling the two semiconductors reduces recombination through efficient electron transfer from Fe_2O_3 to ZnO, thus justifying the observed photocatalytic activity results [23].

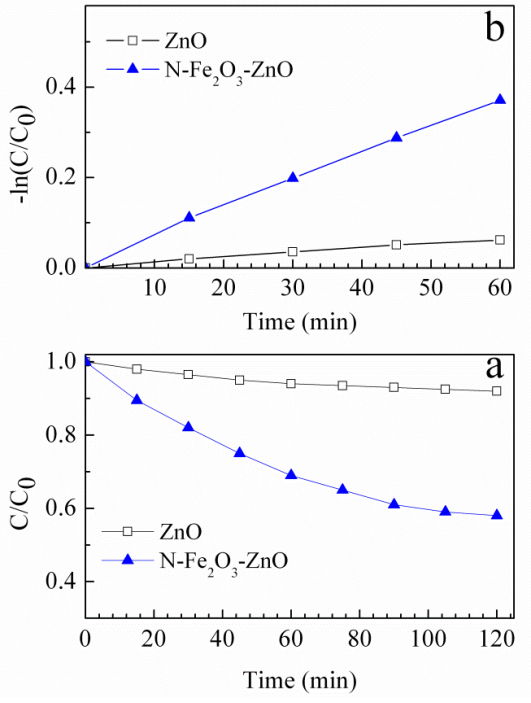

Fig. 6. (a) Degree of decolourisation of Methyl Orange dye and (b) dependence of the rate constants of photocatalytic decolourisation of Methyl Orange over pure ZnO and mechanochemically synthesised N-Fe_2O_3-ZnO samples under visible light irradiation.

Some researchers have reported that the kinetic behaviour of photocatalytic reaction can be described by a pseudo-first order model. It has been noted that the plot of $\ln(C_0/C)$ versus illumination time represents a straight line and the slope of linear regression can be equal to the apparent pseudo-first order rate constant k. The rate constants for the mechanochemically synthesised N-Fe_2O_3-ZnO and pure ZnO samples were 0.372 and 0.06 h^{-1}, respectively. These results indicated that the localised electron states of Fe_2O_3 serve as charge carrier traps for photogenerated charge carriers under visible light irradiation [32]. According to the literature, the trapped electron or hole will be migrated to the catalyst surface where it will participate in a redox reaction with the dye molecules, thereby suppressing the electron-hole recombination and hence substantially increasing the photodecolourisation efficiency [33].

Furthermore, it is suggested that the different photocatalytic activity behaviours depend on several factors such as crystallite size and band gap. According to the XRD measurements in the present study N-dopant and Fe_2O_3 in mechanochemically prepared samples led to reduction of the crystallite size. In large crystallites of ZnO, recombination is dominant and can be inhibited by decreasing the particle size by ball milling. The pronounced photocatalytic effect is ascribed to the reduced band gap (DRS) and lower recombination rate (PL) of ZnO.

CONCLUSION

In this study, N-doped Fe_2O_3-ZnO photocatalyst was prepared by a combination of mechanochemical/thermal treatment and was used as a catalyst in the process of photodecolourisation of Methyl Orange as a dye model. A lower PL intensity of the mechanochemically synthesised samples in comparison with the initial ZnO indicated a lower recombination rate of excited electrons and holes. Initial ZnO possessed low PL intensity under visible light irradiation. The mechanochemically synthesised samples exhibited a higher photocatalytic decolourisation of Methyl Orange under visible light in comparison with initial ZnO, indicating that visible light generates photon-induced electrons and holes in N-doped Fe_2O_3-ZnO due to appearance of electron level in the band gap. The visible light responsive photocatalyst showed effective activity in the decolourisation process of Methyl Orange and up to 42% for 120 min by increasing the doping level.

Acknowledgment: *The authors are grateful to the Bulgarian National Science Fund for financial*

support under project DNTS/Slovakia 01/2 and to the Slovak Research and Development Agency for contracts SK-BG-2013-0011 and 14-0103. M.F. thanks VEGA (project 2/0128/16).

REFERENCES

1. M. Janczarek, E. Kowalska, *Catalysts*, **7**, 317 (2017).
2. W. Chiron, A. Fernandes-Cilba, A. Rodriguez, E. Garcia-Calvo, *Water Res*., **34,** 366 (2000).
3. K. M. Lee, Ch. W. Lai, K. S. Ngai, J. Ch. Juan, *Water Res*., **88**, 428 (2016).
4. A. di Mauro, M. E. Fragala, V. Privitera, *Mat. Sci. Semicon. Proc.*, **69**, 44 (2017).
5. C. Tian, Q. Zhang, A. Wu, M. Jiang, Z. Liang, *Chem. Commun*., **48**, 2858 (2012).
6. Z. Wang, Y. Liu, B. Huang, Y. Dai, Z. Lou, G. Wang, X., Zhang, X. Qin, *Phys. Chem. Chem. Phys*., **16**, 2758 (2014).
7. K. Mageshwari, D. Nataraj, T. Pal, R. Sathymoorthy, J. Park, *J. Alloys Comp*., **625**, 362 (2015).
8. G. T. S. T. da Silva, K. T. G. Carvalho, O. F. Lopes, E. S. Gomes, A. R. Maliagutti, V. R. Mastelaro, C. Ribeiro, H. A. J. L. Mourao, *Chemcatchem*, **9**, 3795 (2017).
9. P. S. Bassi, L. H. Wong, J. Barber, *Phys. Chem. Chem. Phys*., **16**, 11834 (2014).
10. M. Mishra, D.-M. Chun, *Appl. Catal. A: General* **498**, 126 (2015).
11. S. Balachandran, M. Swaminathan, *J. Phys. Chem. C*, **116**, 26306 (2012).
12. M. Dorraj, M. Alizadeh, N. A. Sairi, W. J. Basirun, B. T. Goh, P. M. Woi, Y. Alias, *Appl. Surface Sci*., **414**, 251 (2017).
13. K. Madeshwari, D. Nataraj, T. Pal, R. Sathyamoorthy, J. Park, *J. Alloys Comp*. **625**, 362 (2015).
14. R. K. Sharma, D. Kumar, R. Ghose, *Ceram. Int.*, **42**, 4090 (2016).
15. V. Sepelak, A. Duvel, M. Wilkening, K. D. Becker, *Chem. Soc. Rev*., **42**, 7507 (2013).
16. M. P. Tsvetkov, K. L. Zaharieva, Z. P. Cherkezova-Zheleva, M. M. Milanova, I. G. Mitov, *Bulg. Chem. Commun*., **47**, 354 (2015).
17. V. Polliotto, E. Albanese, S. Livraghi, G. Pacchioni, E. Giamello, *J. Mater. Chem. A*, **5**, 13062 (2017).
18. W. Wang, M. O. Tade, Z. Shao, *Prog. Mater. Sci.*, **92**, 33 (2018).
19. K. Jiratova, A. Spojakina, L. Kaluza, R. Palcheva, J. Balabanova, G. Tyuliev, *Chinese J. Catal*., **37**, 258 (2016).
20. D. R. Cummins, H. B. Russell, J. B. Jasinski, M. Menon, K. M. Sunkara, *Nano Lett*., **13**, 2423 (2013).
21. T. Žák, Y. Jirásková, CONFIT: Mössbauer spectra fitting program, *Surf. Interface Anal.*, **38**, 710 (2006).
22. V. I. Iliev, D. V. Tomova, V. F. Georgiev, S. K. Rakovski, *Bulg. Chem. Commun*., **49** Special Issue L, 17 (2017).
23. H. Lachheb, F. Ajala, A. Hamrouni, A. Houas, F. Parrino, L. Palmisano, *Catal. Sci. Technol*., **7**, 4041 (2017).
24. M. Anpo, S. Dzwigaj, M. Che, *Adv. Catal*., **52**, 1 (2009).
25. N. S. Portillo-Velez, A. Hernando-Gordillo, M. Bizarro, *Catal. Today*, **287** 106 (2017).
26. M. Scepanovic, T. Sreckovic, K. Vojisavljevic, M. M. Ristic, *Sci. Sinter*., **38**, 169 (2006).
27. H. Ozaki, S. Iwamoto, M. Inoue, *J. Phys. Chem. C***, 111**, 17061 (2007).
28. Y. Cong, J. L. Zhang, F. Chen, M. Anpo, D. N. He, *J. Phys. Chem. C*, **111,** 10618 (2007).
29. T. Tsoncheva, R. Ivanova, M. Dimitrov, D. Paneva, D. Kovacheva, J. Heynych, P. Vomacka, M. Kormunda, N. Velinov, I. Mitov, V. Stengl, *Appl. Catal. A*: *General*, **528**, 24 (2016).
30. S. S. R. Putluru, S. Mossin, A. Riisager, R. Fehrmann, *Catal. Today*, **176**, 292 (2011).
31. H. Kaftelen, K. Ocakoglu, R. Thomann, S. Tu, S. Weber, E. Erdem, *Phys. Rev. B*, **86**, 014113 (2012).
32. L. G. Devi, N. Kottam, B. Narasimha, B. N. Murthy, S. G. Kumar, *J. Mol. Catal. A: Chem.*, **328**, 44 (2010).
33. R. Chauhan, A. Kumar, R. P. Chaudhary, P. Ram, *Spectrochim. Acta Part A: Mol. Biomol. Spectrosc.*, **98**, 256 (2012).

СВОЙСТВА НА МЕХАНОХИМИЧНО СИНТЕЗИРАН ДОТИРАН С АЗОТ Fe_2O_3-ZnO СМЕСЕН ОКСИД

Н. Г. Костова*[1], М. Фабиан[2], Е. Дуткова[2], Н. Велинов[1], Й. Каракирова[1], М. Балаж[2]

[1] *Институт по катализ, Българска академия на науките, 1113 София, България*
[2] *Институт по геотехника, Словашка академия на науките, 04001 Кошице, Словакия*

Постъпила на: 2 февруари 2018 г.; Преработена на: 13 април 2018 г.

(Резюме)

Настоящата статия се отнася до получаването и охарактеризирането на дотиран с азот Fe_2O_3-ZnO смесен оксид и способността на този материал да обезцвети органичното багрило Метил Оранж във воден разтвор при облъчване с видима светлина. Фотокаталитичният материал беше получен чрез екологичен механохимичен метод на синтез. Фотокатализаторите бяха охарактеризирани с рентгенофазов анализ (РФА), УВ-видима дифузно-отражателна спектроскопия (ДОС), фотолуминесцентна спектроскопия (ФЛ), електронен парамагнитен резонанс (ЕПР) и Мьосбауерова спектроскопия. РФА показа, че прилагането на механохимичен синтез промотира промени в размера на кристалитите. Беше регистрирано стесняване на забранената зона на механохимично синтезирания дотиран с азот Fe_2O_3-ZnO смесен оксид и подобряване на фотокаталитичната активност при облъчване с видима светлина в сравнение с изходния ZnO. Пониженият интензитет във фотолуминесцентния спектър на N-Fe_2O_3-ZnO свидетелства за подобрено разделяне на зарядите, по-ниска скорост на рекомбиниране на електрон-дупка и съответно по-висока фотокаталитична активност в сравнение с изходния ZnO.